

Two ion species studies in LAPD*
Ion-ion Hybrid Alfvén Wave Resonator

G. J. Morales, S. T. Vincena, J. E. Maggs and W. A. Farmer

UCLA

Experiments performed at the Basic Plasma Science Facility (BaPSF)

Sponsored by: ONR-MURI

***S. T. Vincena, G. J. Morales and J. E. Maggs, Physics of Plasmas 17, 052106 (2010)**

Motivation

- **Shear Alfvén waves in two-ion species plasmas (a.k.a. ion cyclotron waves, EMIC, ion-hybrid waves etc..) interact strongly with ions**

- **Altitude-sensitive noise detected by spacecraft in H^+ - He^+ geoplasma**

5. M. Temerin and R.L. Lysak, *J. Geophys. Res.* 89, 2849 (1984).

- **Ion acceleration in solar corona**

6. K. G. McClements and L. Fletcher, *Astrophys. J.* 693, 1494 (2009).

- **Possible wave resonators in equatorial region of planetary magnetospheres----RESONANCE MISSION**

7. A.V. Gigliemi, A.S. Potapov, and C.T. Russell, *Pis'ma v ZhETF* 72, 432 (2000).

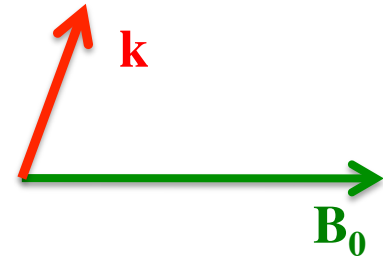
8. A. G. Demekhov, V. Y. Trakhtengerts, M. M. Mogilevsky, and L. M. Zelenyi
Adv. Space Res. 32, 355 (2003).

Essential Physics--I

For small transverse scales the **compressional mode is evanescent**

Shear Alfvén wave **dispersion relation is well approximated by**

$$k_{\parallel}^2 = \left(\frac{\omega}{c}\right)^2 \epsilon_{\perp} \left[1 - \left(\frac{k_{\perp} c}{\omega}\right)^2 \frac{1}{\epsilon_{\parallel}} \right]$$



For **two cold ion species**

$$\epsilon_{\perp} \approx \frac{\omega_{p1}^2}{\Omega_1^2 - \omega^2} + \frac{\omega_{p2}^2}{\Omega_2^2 - \omega^2}$$

Perpendicular **dielectric vanishes at**

$$\omega_{ii} = \sqrt{\frac{\omega_{p1}^2 \Omega_2^2 + \omega_{p2}^2 \Omega_1^2}{\omega_{p1}^2 + \omega_{p2}^2}}$$

and singular at $\omega = \Omega_1$ and $\omega = \Omega_2$

Essential Physics--II

Frequency ω and k_{\perp} are set by source

Axial cut-off occurs when $\varepsilon_{\perp} = 0$

For cold ions at $\omega = \sqrt{\frac{\omega_{p1}^2 \Omega_2^2 + \omega_{p2}^2 \Omega_1^2}{\omega_{p1}^2 + \omega_{p2}^2}} \equiv \Omega_{ii}$

But when $k_{\perp} \rho_i$ is not negligible

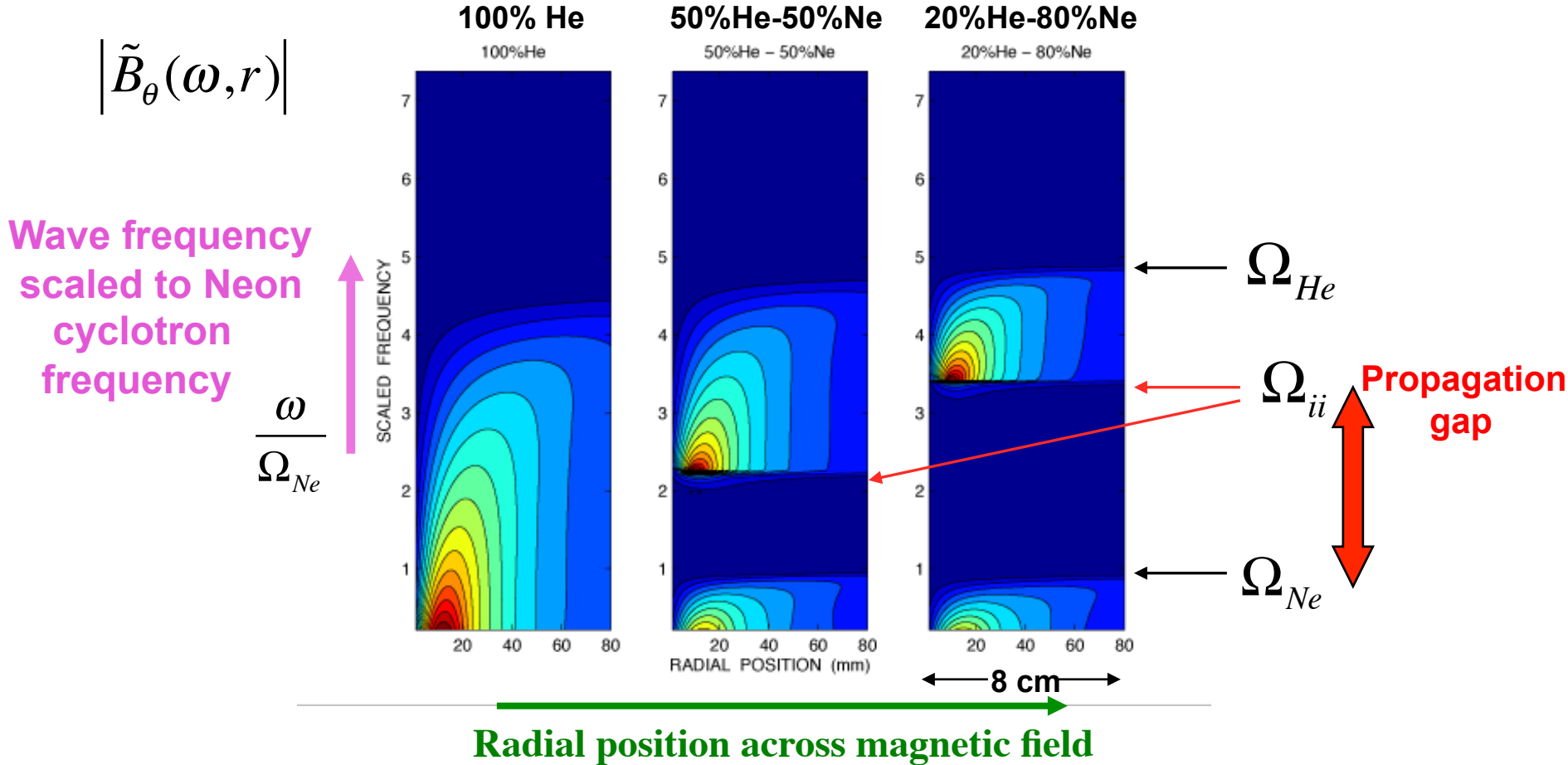
$$\varepsilon_{\perp} = 1 + \left(\frac{\omega_{pe}}{\Omega_e} \right)^2 - 2 \sum_s \left(\frac{\omega_{ps}}{k_{\perp} \rho_s} \right)^2 \sum_{l=1}^{\infty} \frac{e^{-(k_{\perp} \rho_s)^2} I_l(k_{\perp}^2 \rho_s^2)}{\omega^2 - (l \Omega_s)^2}$$

Vanishes at frequencies corresponding to “pure” IBW

Consequence: shear Alfvén wave experiences multiple propagation bands between the lower and the higher cyclotron frequencies that become more pronounced at large ion temperatures or small transverse scales

Effect of Species (He/Ne) Concentration for Cold Ions

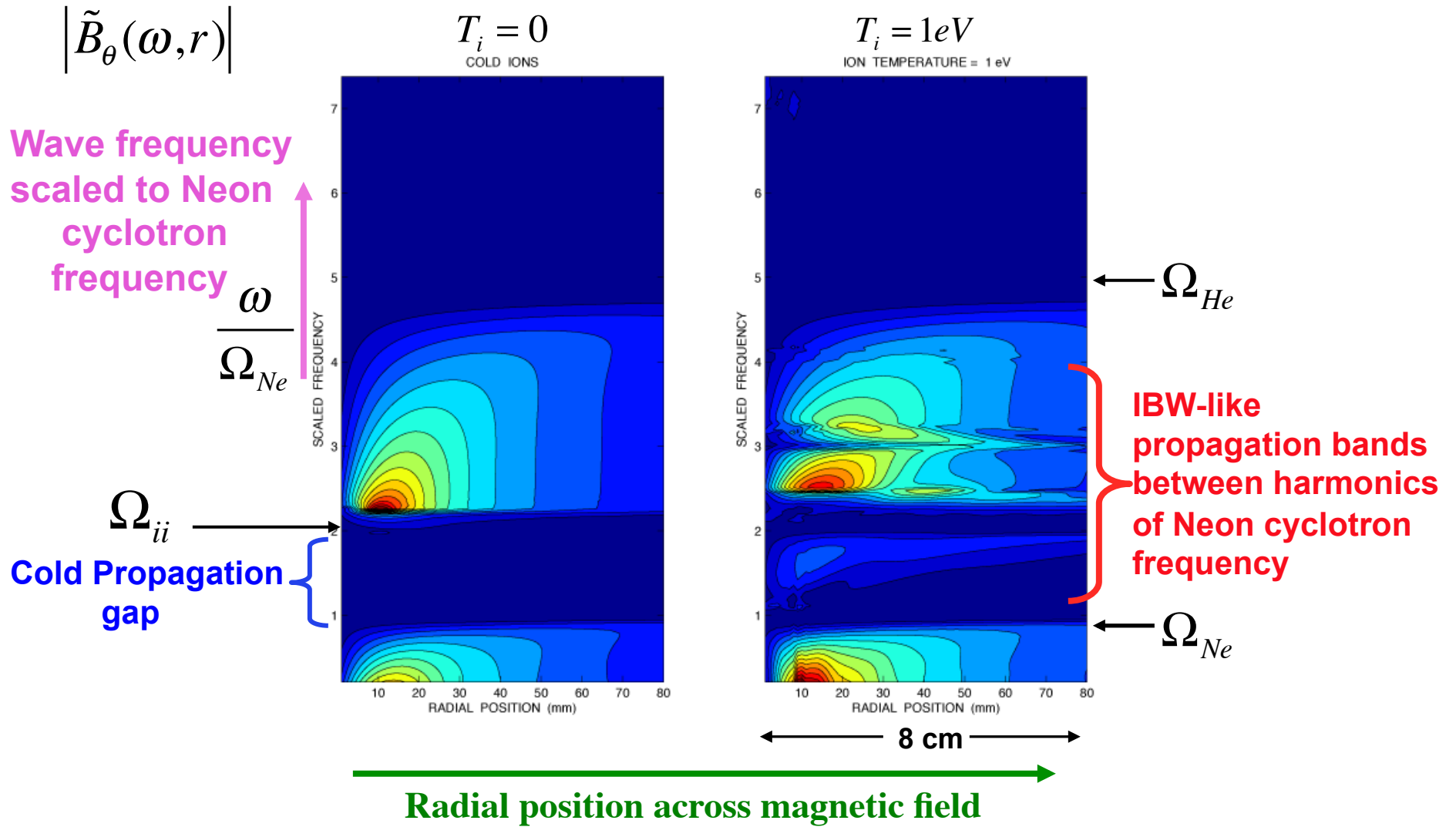
Contour in “frequency-radial position space” at fixed axial location $z = 4 \text{ m}$



Typical LAPD parameters $N_e = 10^{12} \text{ cm}^{-3}$; $B_0 = 750 \text{ G}$; $T_e = 5 \text{ eV}$; $T_i = 0$; $a = 1 \text{ cm}$

Modification of Cold Propagation Gap by Ion Temperature

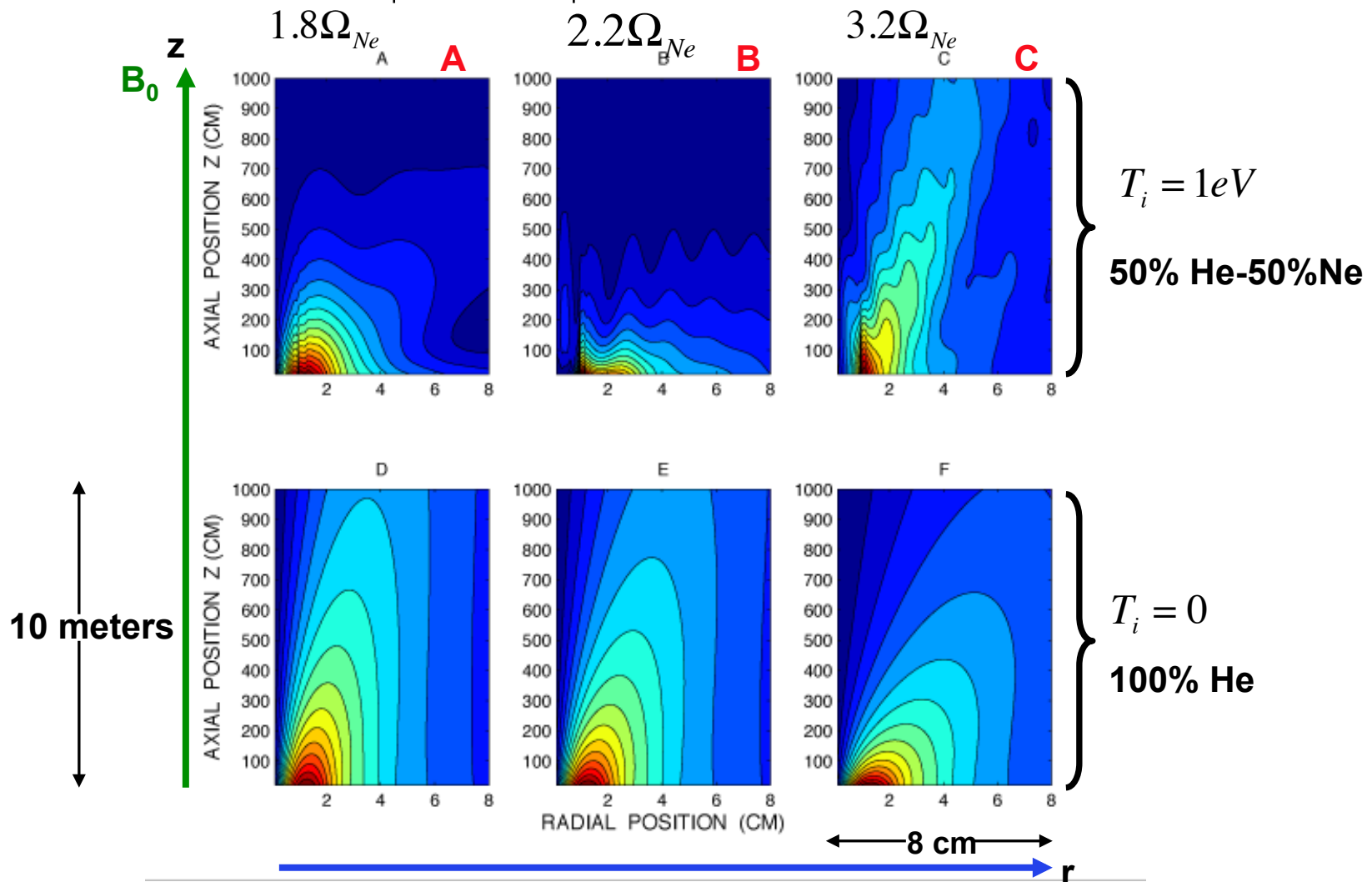
Contour in “frequency-radial position space” at fixed axial location $z = 4$ m



Typical LAPD parameters $N_e = 10^{12} \text{ cm}^{-3}$; $B_0 = 750 \text{ G}$; $T_e = 5 \text{ eV}$; 50%He-50%Ne; $a = 1 \text{ cm}$

Comparison of Spatial Pattern (z, r) for Different Frequencies

Contour of $|\tilde{B}_\theta(\omega, z, r)|$ for fixed frequencies

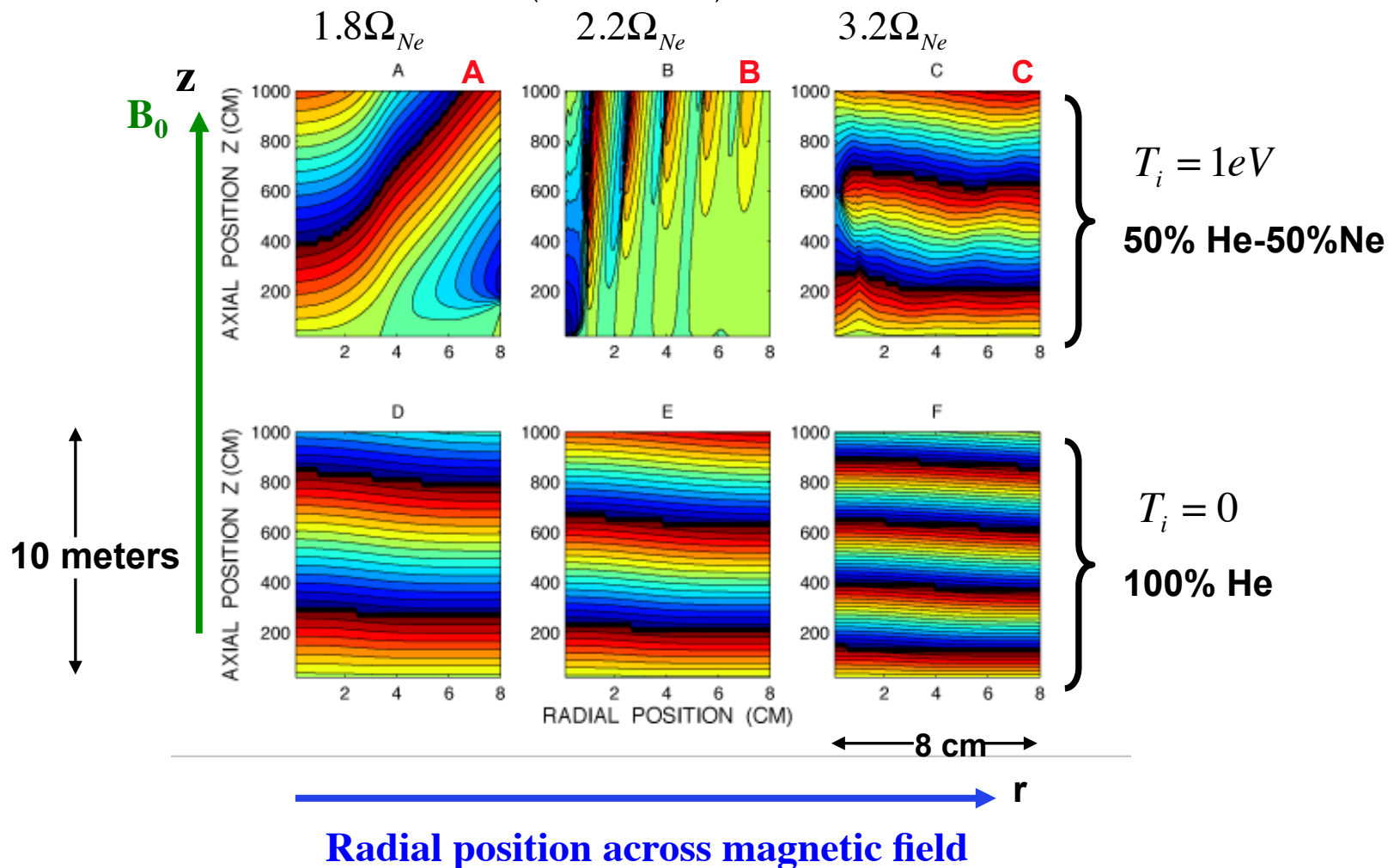


Radial position across magnetic field

Typical LAPD parameters $N_e = 10^{12} \text{ cm}^{-3}$; $B_0 = 750 \text{ G}$; $T_e = 5 \text{ eV}$; $a = 1 \text{ cm}$

Comparison of Spatial Phase-Pattern (z, r) for Different Frequencies

Contour of $\arg(\tilde{B}_\theta(\omega, z, r))$ for fixed frequencies

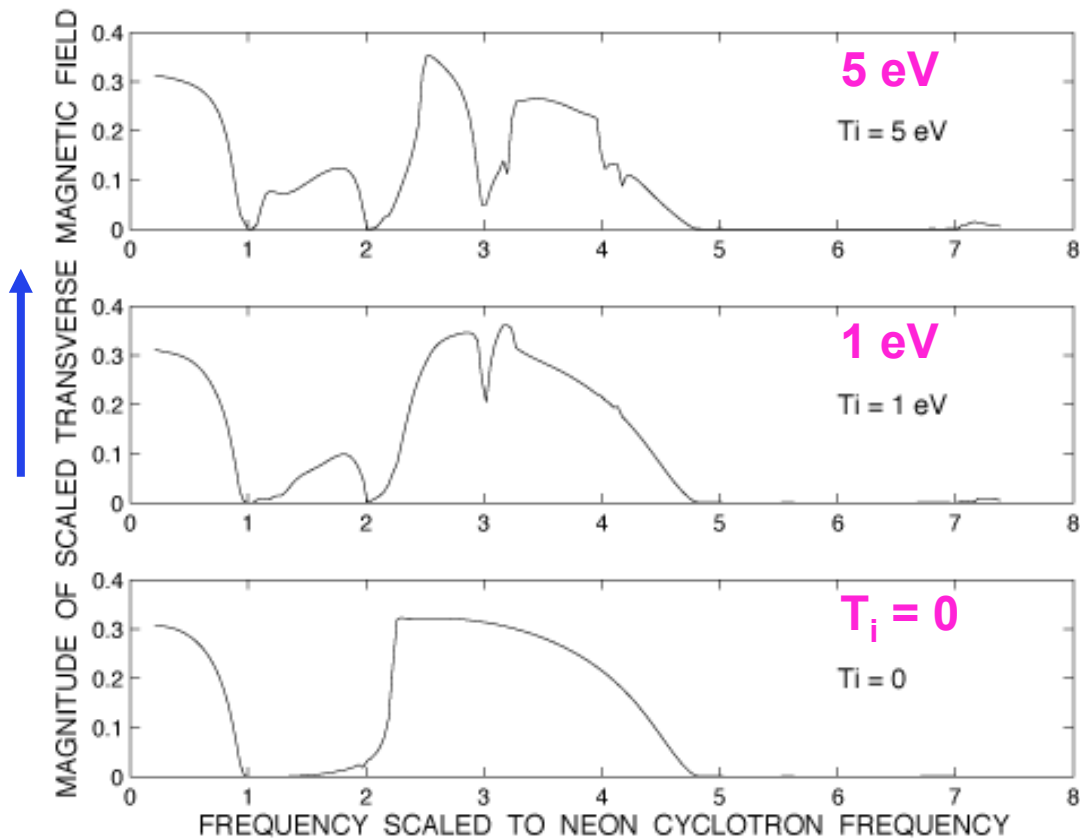


Typical LAPD parameters $N_e=10^{12} \text{ cm}^{-3}$; $B_0 = 750 \text{ G}$; $T_e = 5 \text{ eV}$; $a = 1 \text{ cm}$

Effect of Increasing Ion temperature

Frequency dependence of $|\tilde{B}_\theta(\omega, r, z)|$ at a fixed position
 $z = 4$ meters, $r = 3$ cm

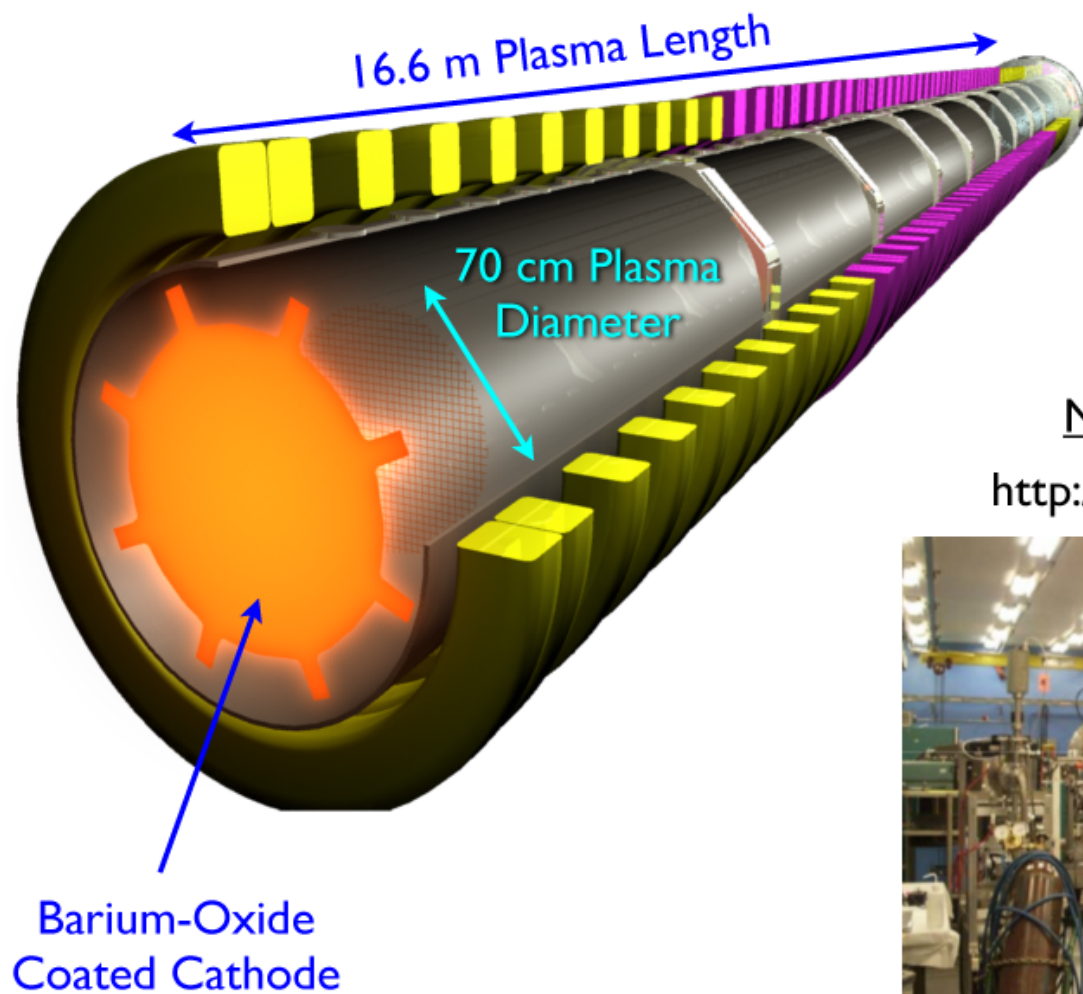
Magnitude of
 azimuthal
 magnetic field



Scaled frequency $\frac{\omega}{\Omega_{Ne}}$ \longrightarrow

Typical LAPD parameters $N_e = 10^{12} \text{ cm}^{-3}$; $B_0 = 750 \text{ G}$; $T_e = 5 \text{ eV}$; $a = 1 \text{ cm}$; 50%He-50%Ne

Large Plasma Device (LAPD)



Typical Parameters

$$T_e = 5 \text{ eV} \quad n_e = 1-3 \times 10^{12} \text{ cm}^{-3}$$

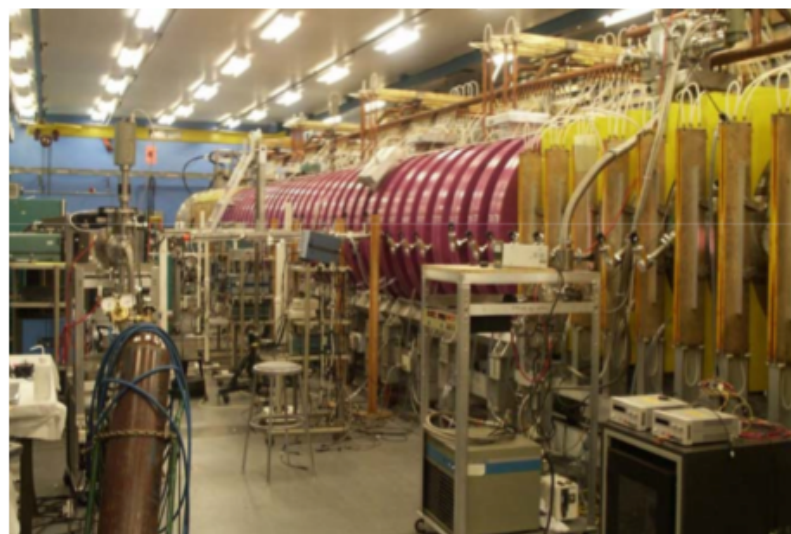
$$T_i = 1 \text{ eV} \quad \tau_{\text{pulse}} = 10 - 12 \text{ ms}$$

$$\text{Rep. Rate} = 1 \text{ Hz}$$

$$B_0 = 500 - 2500 \text{ G}$$

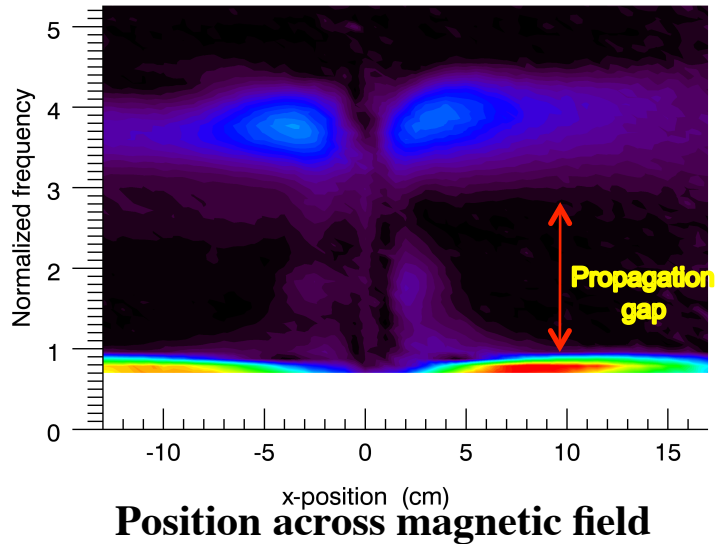
National User Facility

<http://plasma.physics.ucla.edu>

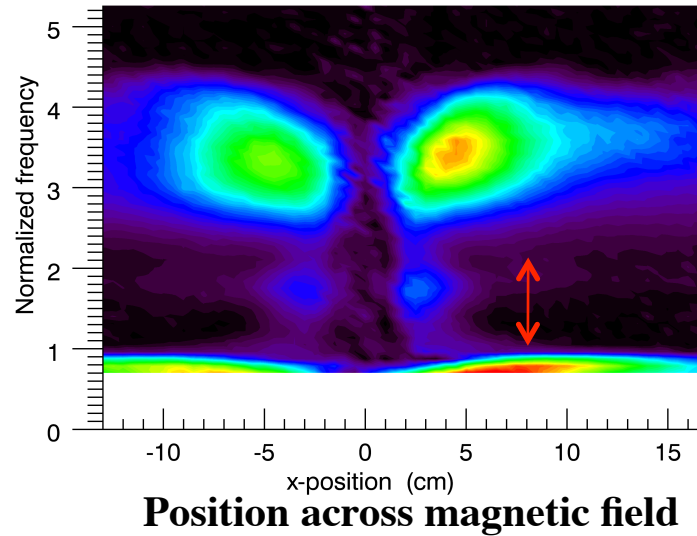


Changing concentration ratio – Helium/Neon mix

30% Helium – 70% Neon

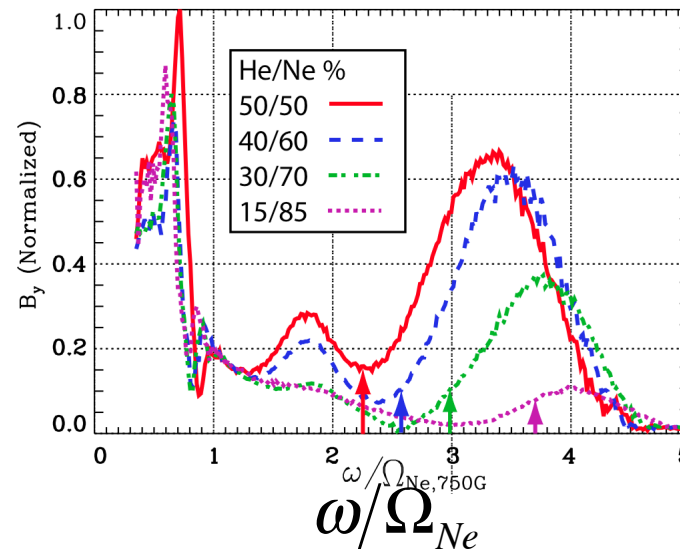


50% Helium – 50% Neon

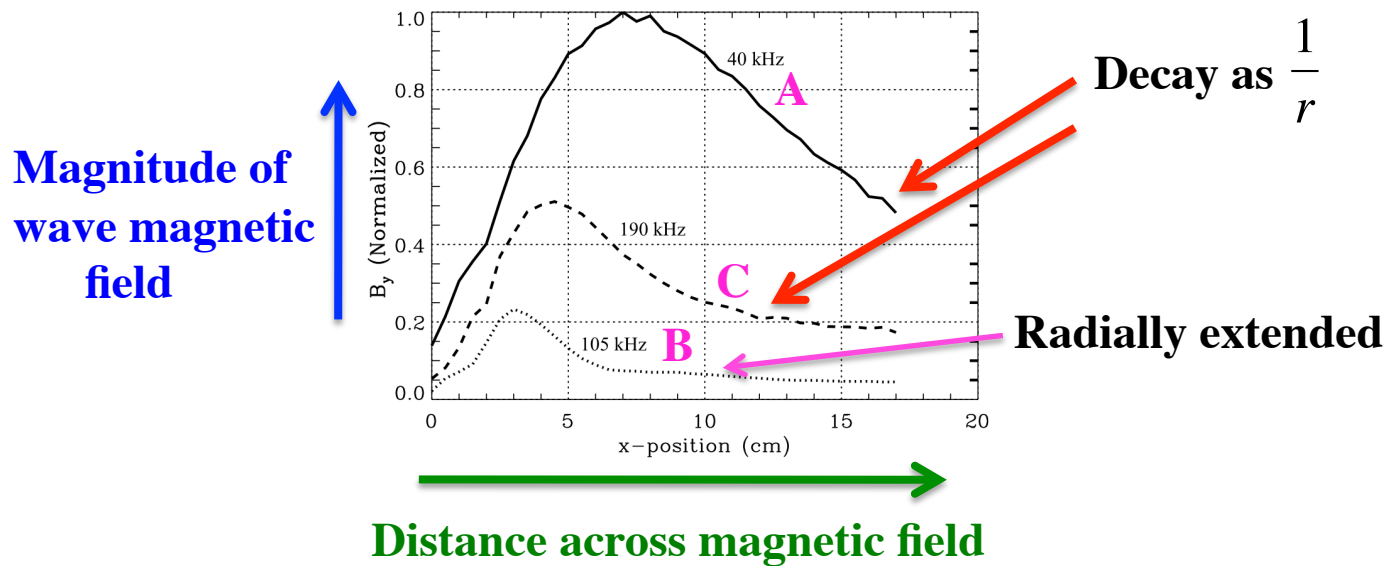
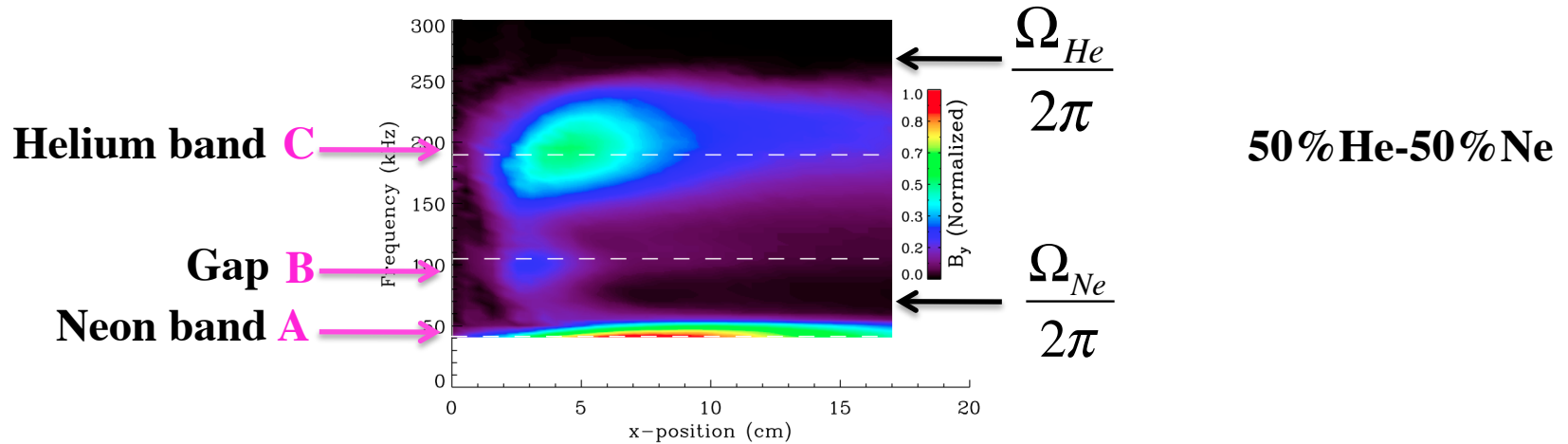


Frequency dependence of magnetic field at $z = 4.8$ m and $r = 2$ cm

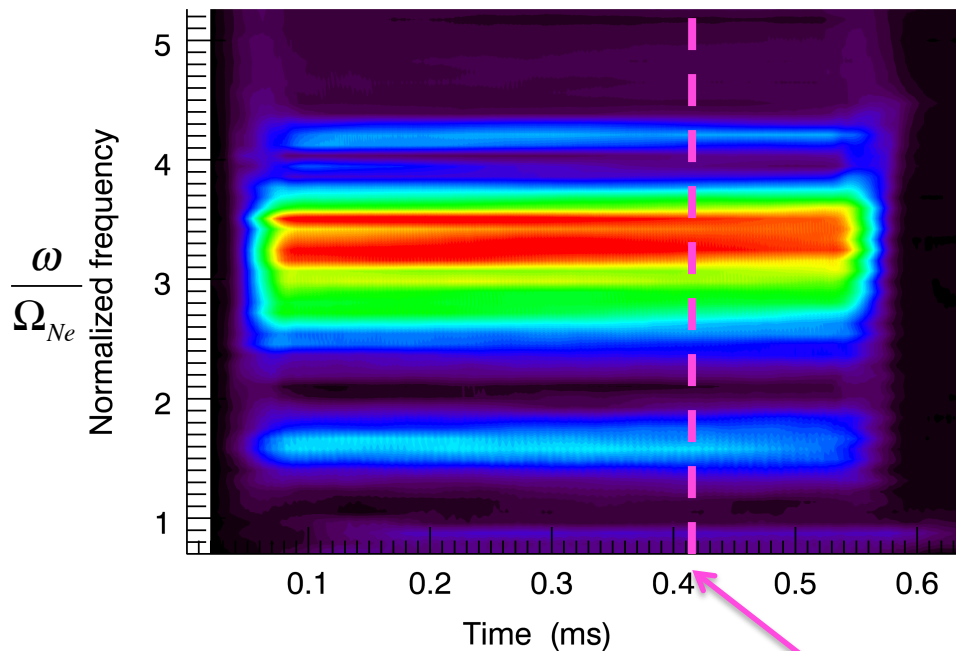
Fig. 9



Measured frequency-radial dependence at fixed $z = 4.8$ m of wave magnetic field



Evidence of IBW-like features



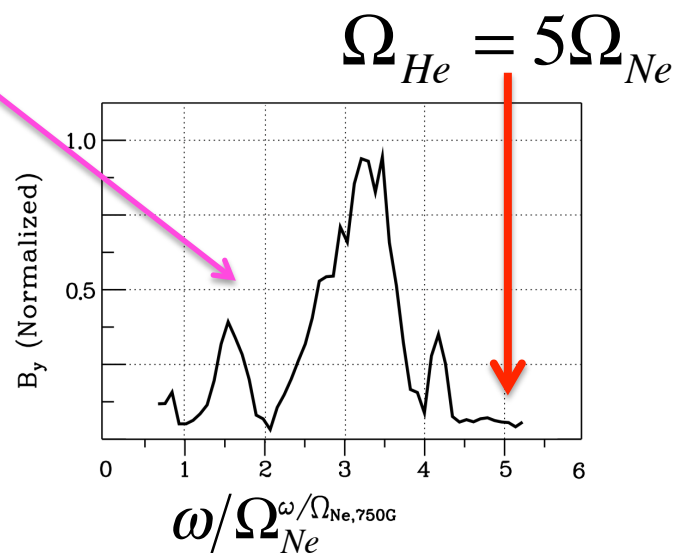
Spectral evolution



(ω, t)

of wave magnetic field
at fixed position

50% He-50% Ne



Essential Physics--III

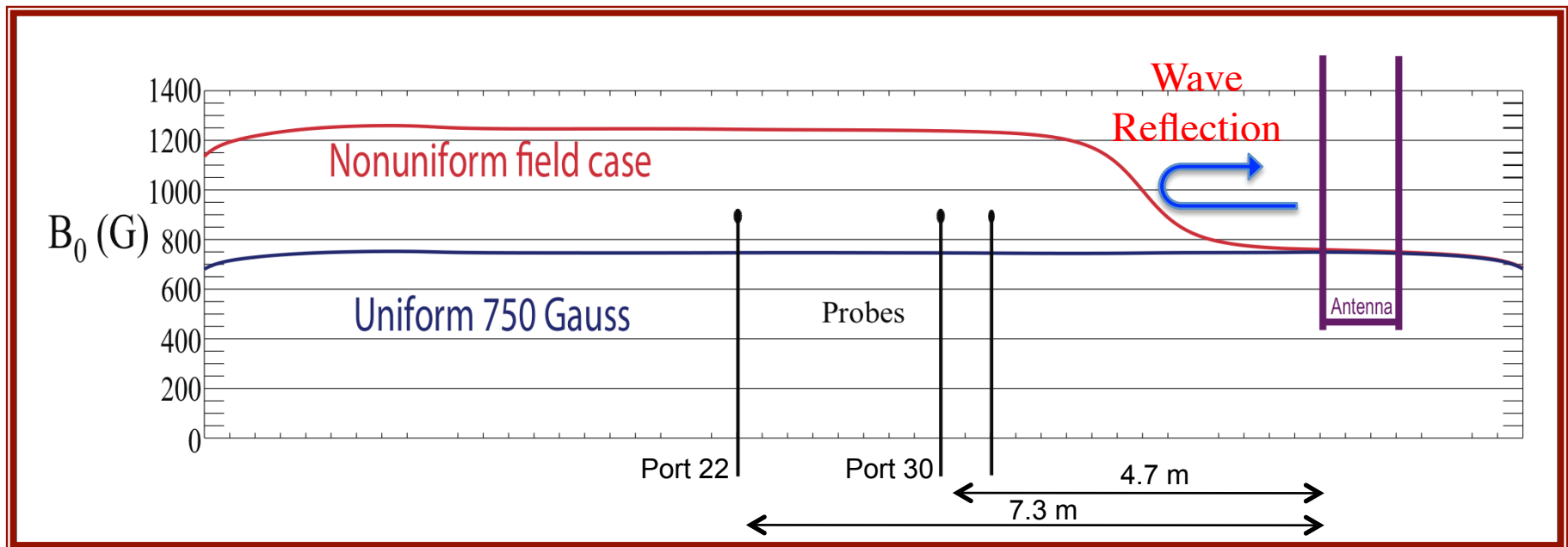
Frequency ω and k_{\perp} are set by source

Axial cut-off occurs when $\epsilon_{\perp} = 0$

For cold ions at $\omega = \sqrt{\frac{\omega_{p1}^2 \Omega_2^2 + \omega_{p2}^2 \Omega_1^2}{\omega_{p1}^2 + \omega_{p2}^2}} = \omega_{ii}$

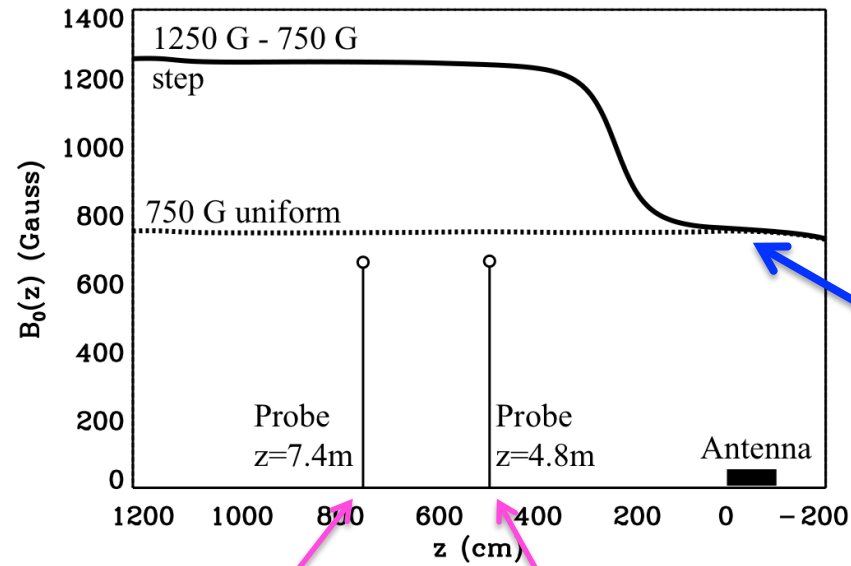
Since $\omega_{ii} \propto B_0(z)$

Waves can be reflected from a magnetic -field ramp



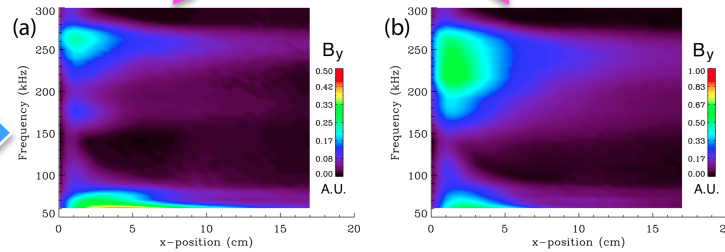
Effect of a magnetic step in a two ion plasma

Experimental configuration



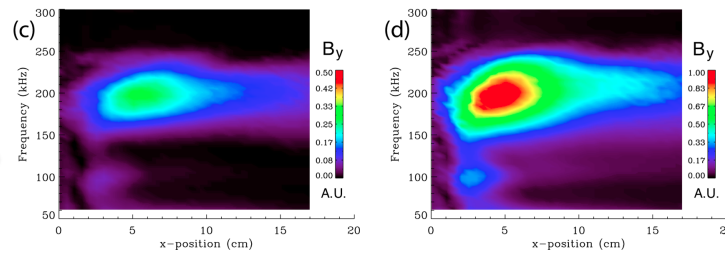
Wave is launched in low field side

With magnetic step

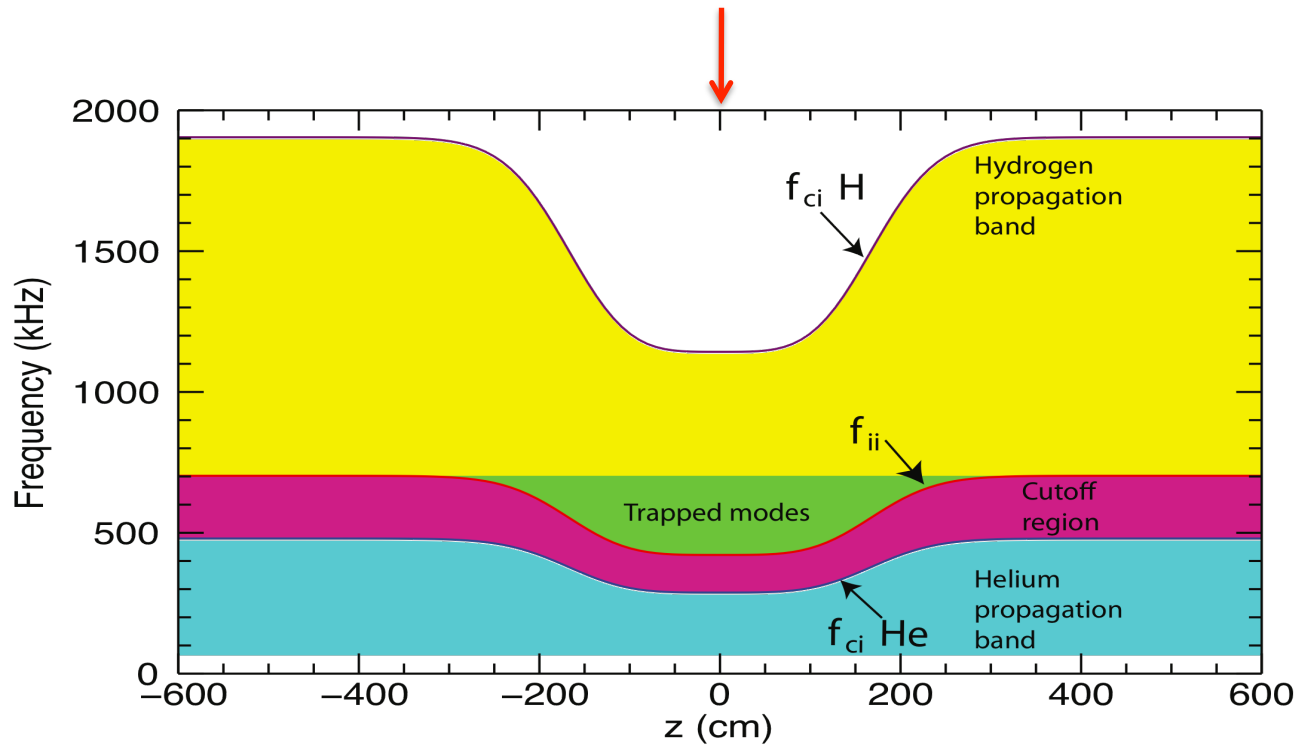
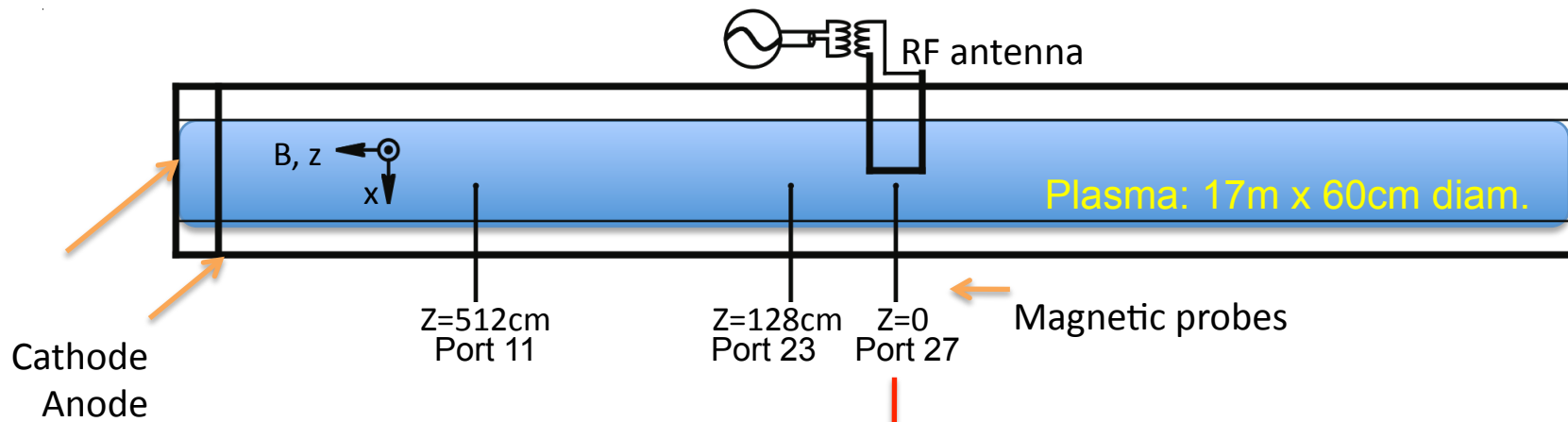


Lower amplitude and no spreading due to evanescence

Uniform field at 750 G



A resonator can be achieved in a magnetic well



H-He plasma

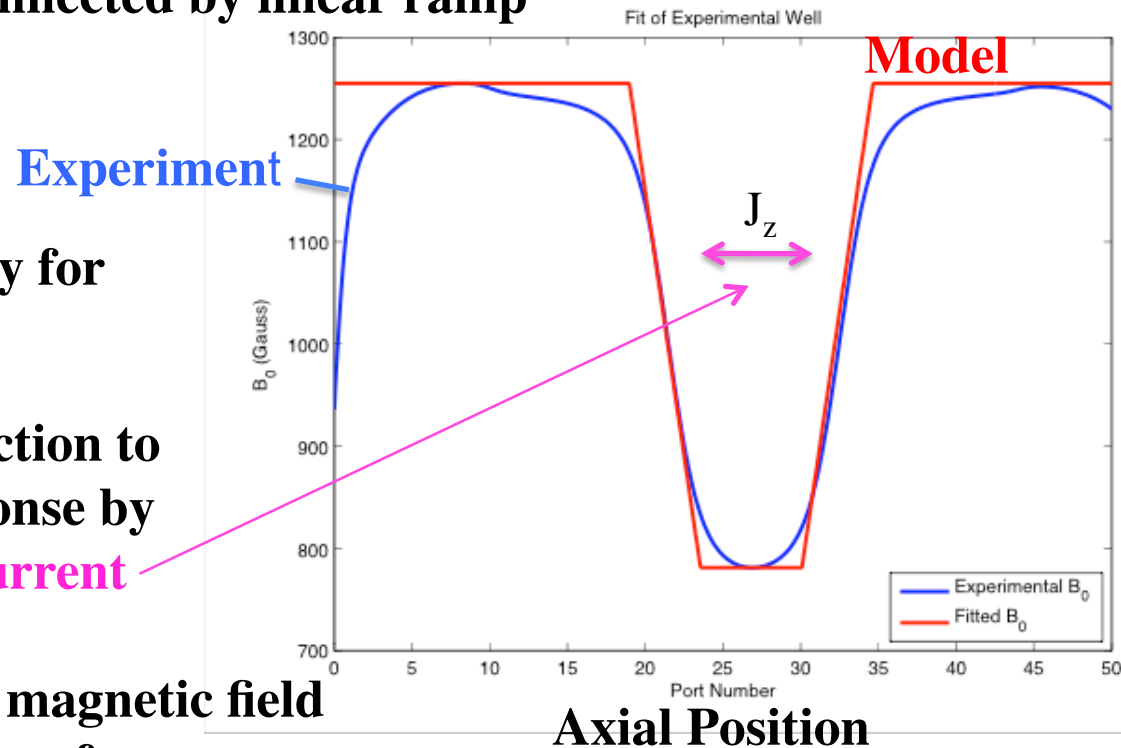
Theoretical Model

1) Approximate **experimental magnetic well** by two uniform regions connected by linear ramp

2) Solve analytically for Green's function

3) Use Green's function to obtain driven response by **straight antenna current**

4) Calculate driven magnetic field as a function of driver frequency

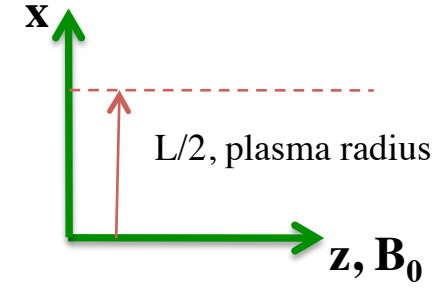


Basic equations in cylindrical geometry (r, z)

$$\frac{\partial^2 E_r}{\partial z^2} - \frac{\epsilon_{\perp}}{\epsilon_{\parallel}} (k_{\perp}^2 - k_0^2 \epsilon_{\parallel}) E_r = -\frac{k_{\perp}}{k_0^2 \epsilon_{\parallel}} \frac{\partial S_z}{\partial z}$$

$$E_z = \frac{1}{k_{\perp}^2 - k_0^2 \epsilon_{\parallel}} \left(S_z - k_{\perp} \frac{\partial E_r}{\partial z} \right)$$

$$B_{\phi} = -\frac{ik_{\perp}}{k_0 (k_{\perp}^2 - k_0^2 \epsilon_{\parallel})} S_z + \frac{ik_0 \epsilon_{\parallel}}{k_{\perp}^2 - k_0^2 \epsilon_{\parallel}} \frac{\partial E_r}{\partial z}$$



$$k_0 \equiv \frac{\omega}{c}$$

$$\mathbf{S} \equiv \frac{4\pi}{c} ik_0 \mathbf{j}$$

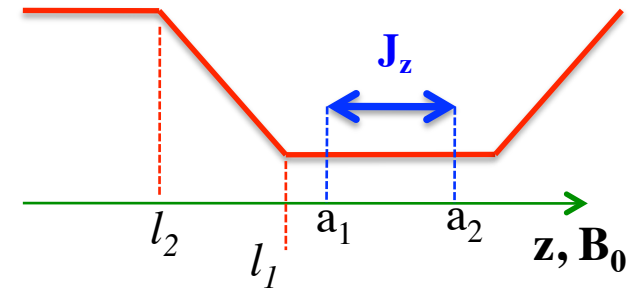
$$\epsilon_{\parallel} = 1 - \frac{\omega_{pe}^2}{\omega(\omega + i\nu_e)}$$

Approximate antenna by a line current source at frequency ω

$$j_z(r, z, t) = \begin{cases} j_0 (\Theta(z - a_1) - \Theta(z - a_2)) e^{-i\omega t} & x < R \\ 0 & \text{otherwise} \end{cases}$$

$$\tilde{j}_z(k_{\perp}, z, t) = \frac{Rj_0}{k_{\perp}} J_1(k_{\perp} R) e^{-i\omega t} (\Theta(z - a_1) - \Theta(z - a_2))$$

$$\frac{\partial S_z}{\partial z} \propto \delta(z - a_1) - \delta(z - a_2)$$



Matching piecewise analytic solutions at 6 axial boundaries

Solution for Fourier component of electric field $\tilde{E}_x(k_\perp, z)$

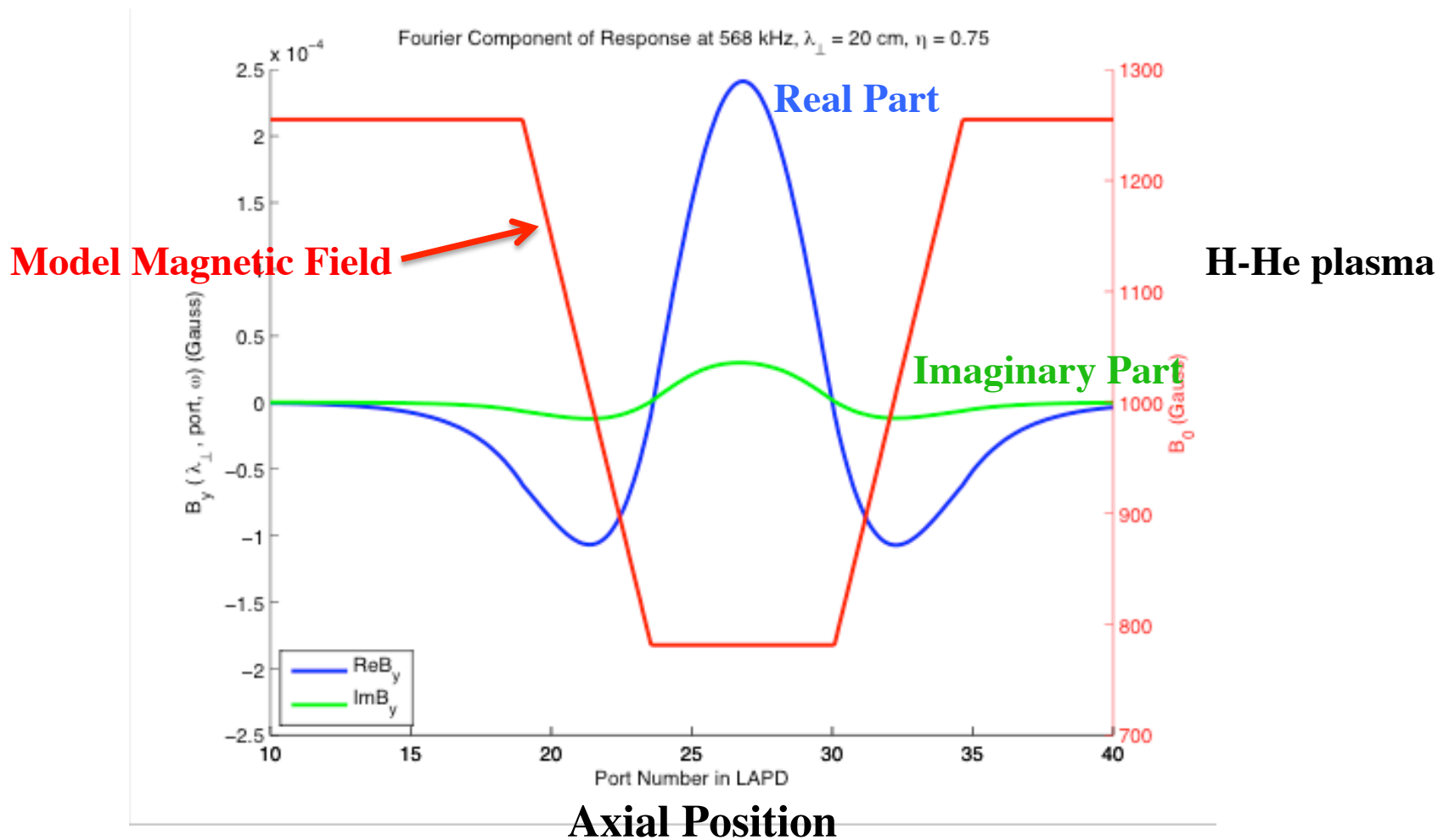
$$\tilde{E}_x(k_\perp, z) = \begin{cases} \text{Outside well} & C_1 e^{k_2(z+l_2)} & z < -l_2 \\ \text{Reflection layer} & C_2 \text{Ai}(-\alpha(z+z_0)) + C_3 \text{Bi}(-\alpha(z+z_0)) & -l_2 < z < -l_1 \\ \text{Left antenna} & C_4 e^{ik_1(z-a)} + C_5 e^{-ik_1(z-a)} & -l_1 < z < a \\ \text{Right antenna} & C_6 e^{ik_1(z-a)} + C_7 e^{-ik_1(z-a)} & a < z < l_1 \\ \text{Reflection layer} & C_2 \text{Ai}(\alpha(z-z_0)) + C_3 \text{Bi}(\alpha(z-z_0)) & l_1 < z < l_2 \\ \text{Outside well} & C_{10} e^{-k_2(z-l_2)} & z > l_2 \end{cases}$$

- Relate B_{\square} to E_r through Faraday's Law, and invert the Hankel transform using antenna spectrum

$$B_\phi(r, z, \omega) = \int_0^\infty \frac{Rj_0}{k_\perp} J_1(k_\perp R) \tilde{B}_\phi(k_\perp, z) J_1(k_\perp r) k_\perp dk_\perp$$

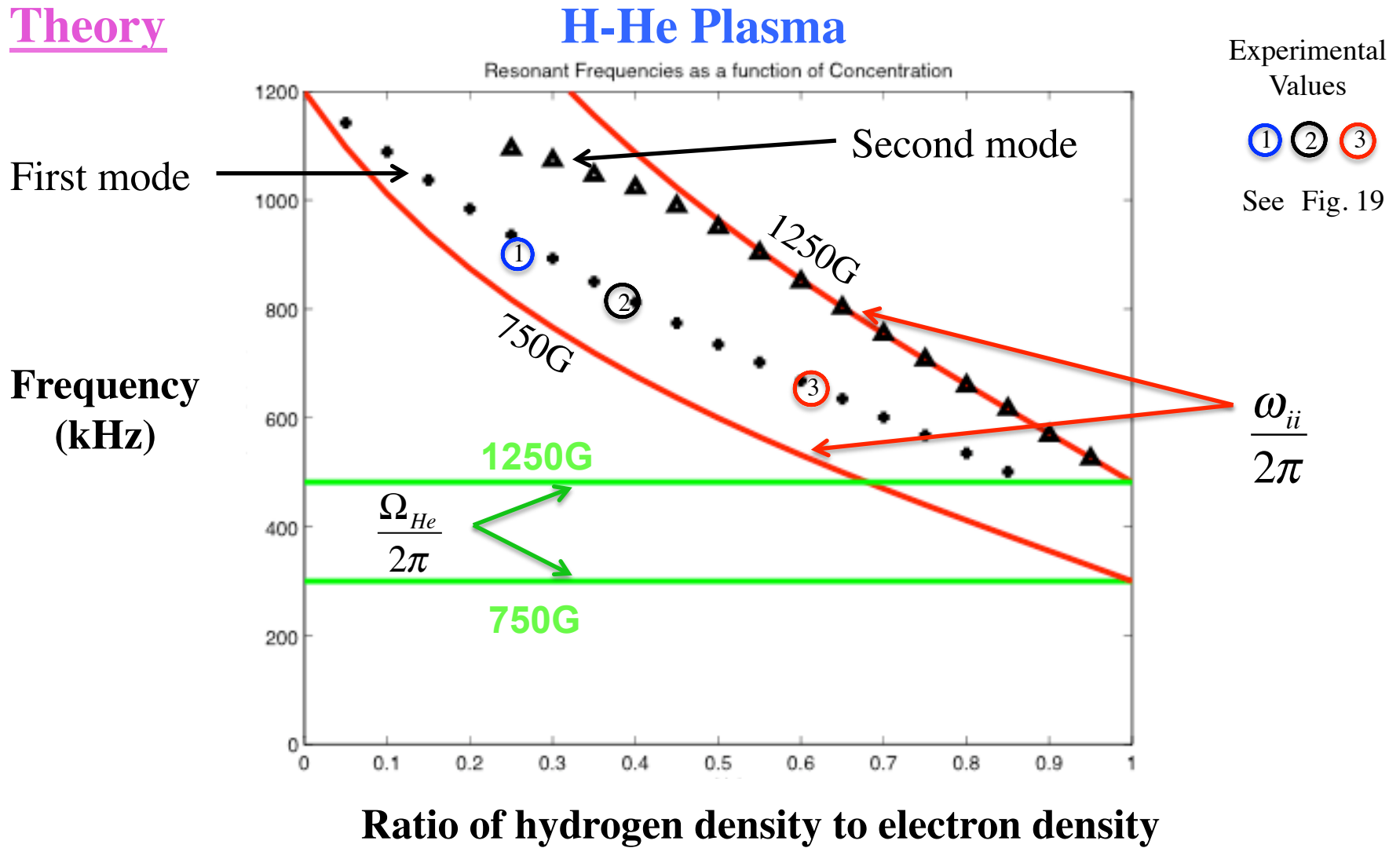
Eigenfunction of Lowest-Frequency Trapped Mode at 568 kHz

Theory



Dependence of trapped mode frequency on concentration ratio

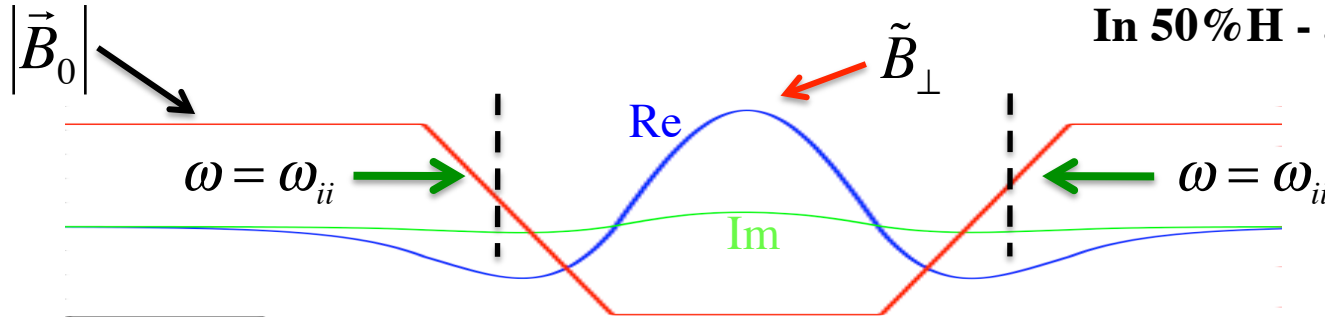
Theory



Resonator eigenmodes excited by a current pulse in a magnetic well

Wave trapping occurs by reflection at ion-ion hybrid resonance

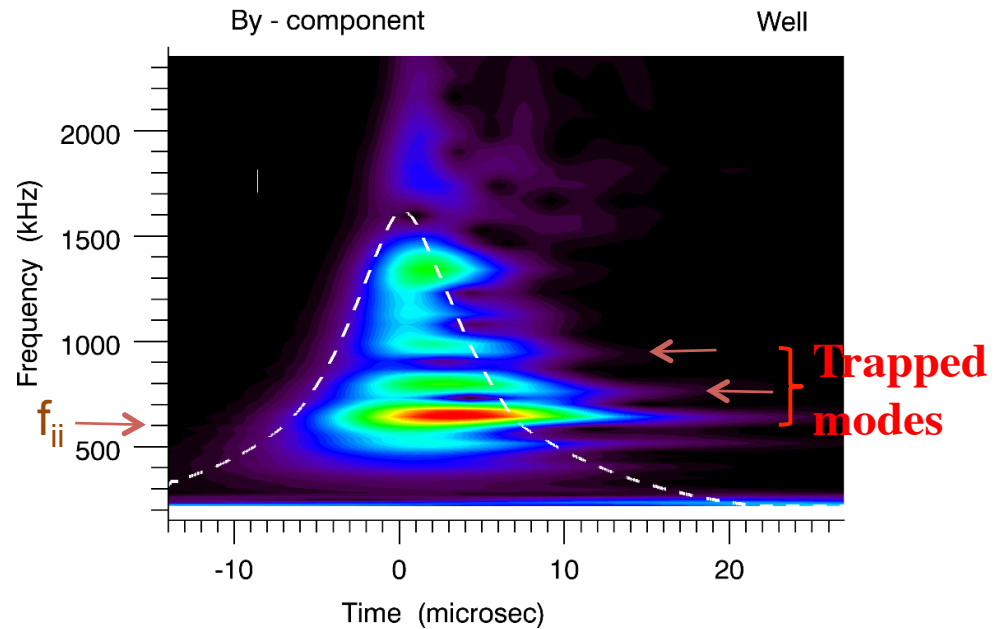
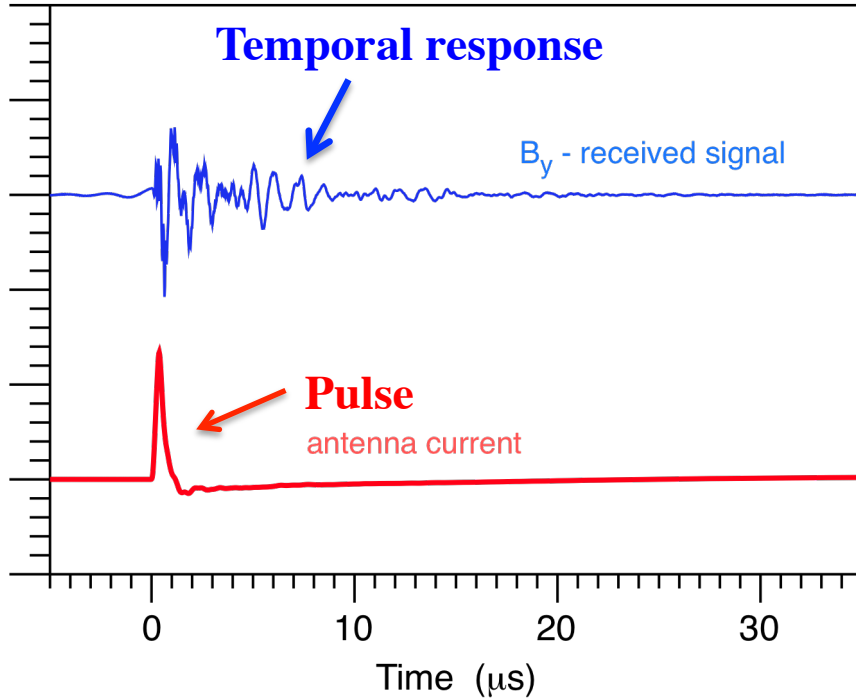
In 50% H - 50% He plasma



Well (750G - 1250G) - Pulse

$r = 10 \text{ cm}$

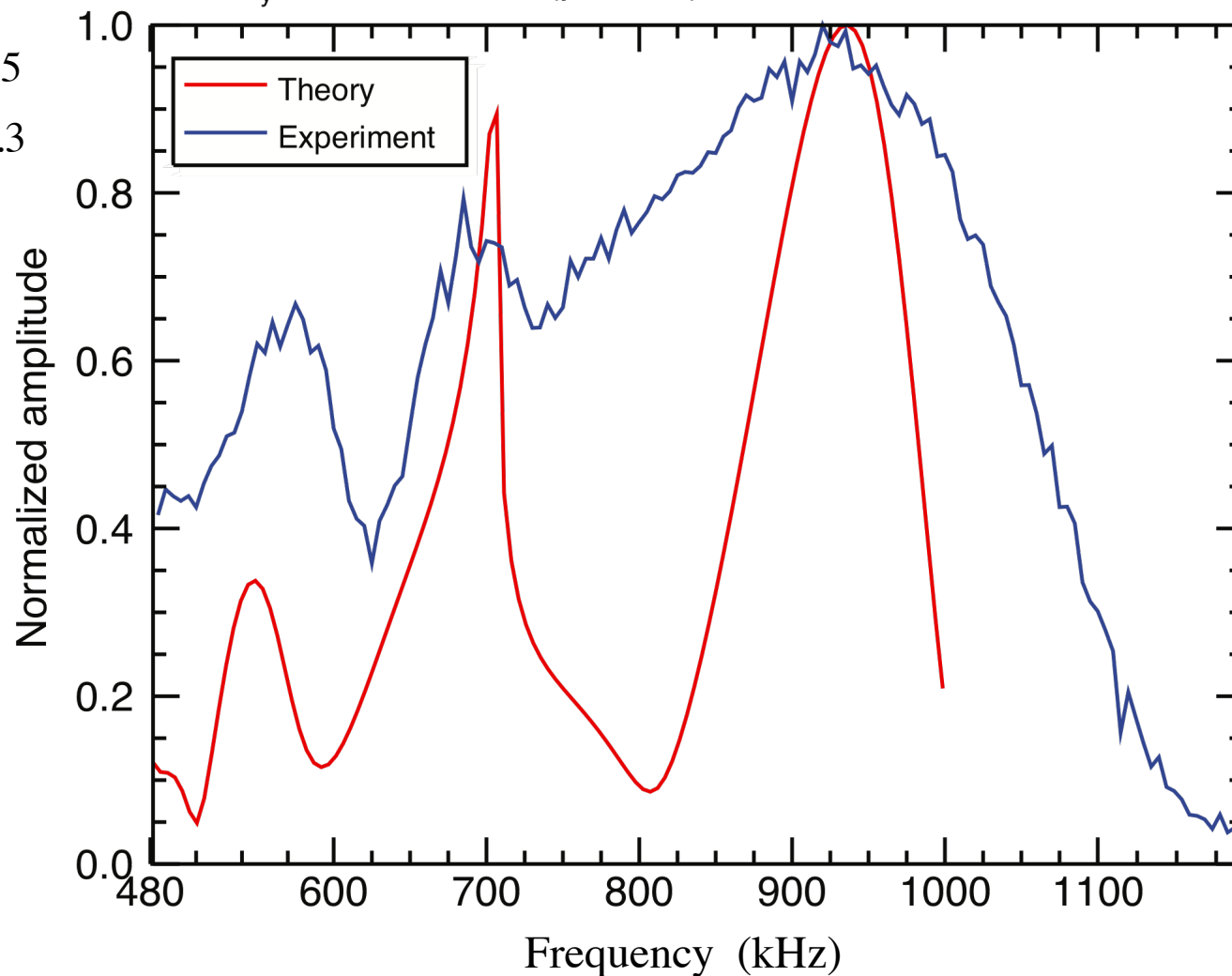
Wavelet analysis



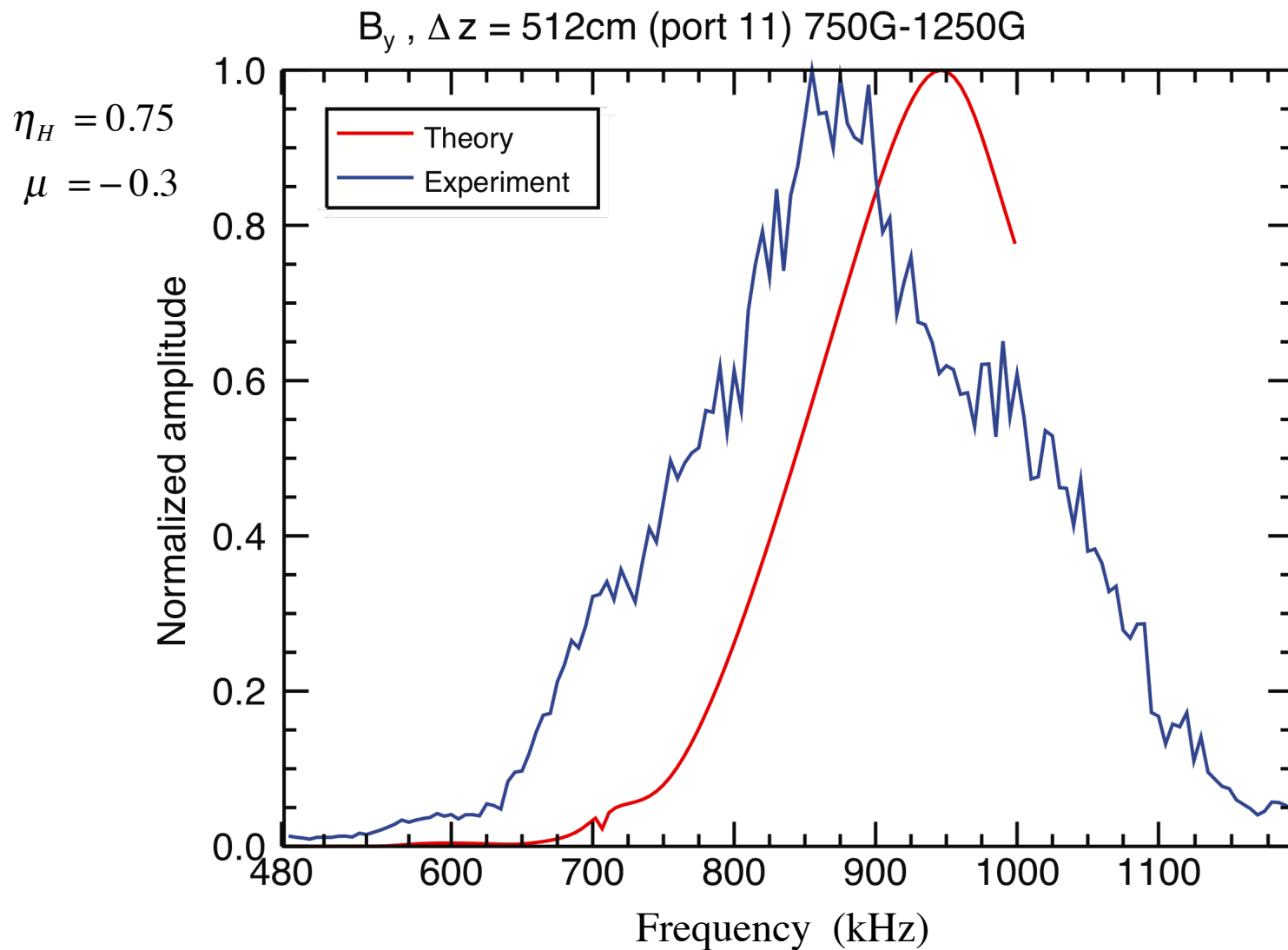
Magnetic field spectra **measured inside** the magnetic well

B_y , $\Delta z = 128\text{cm}$ (port 23) 750G-1250G

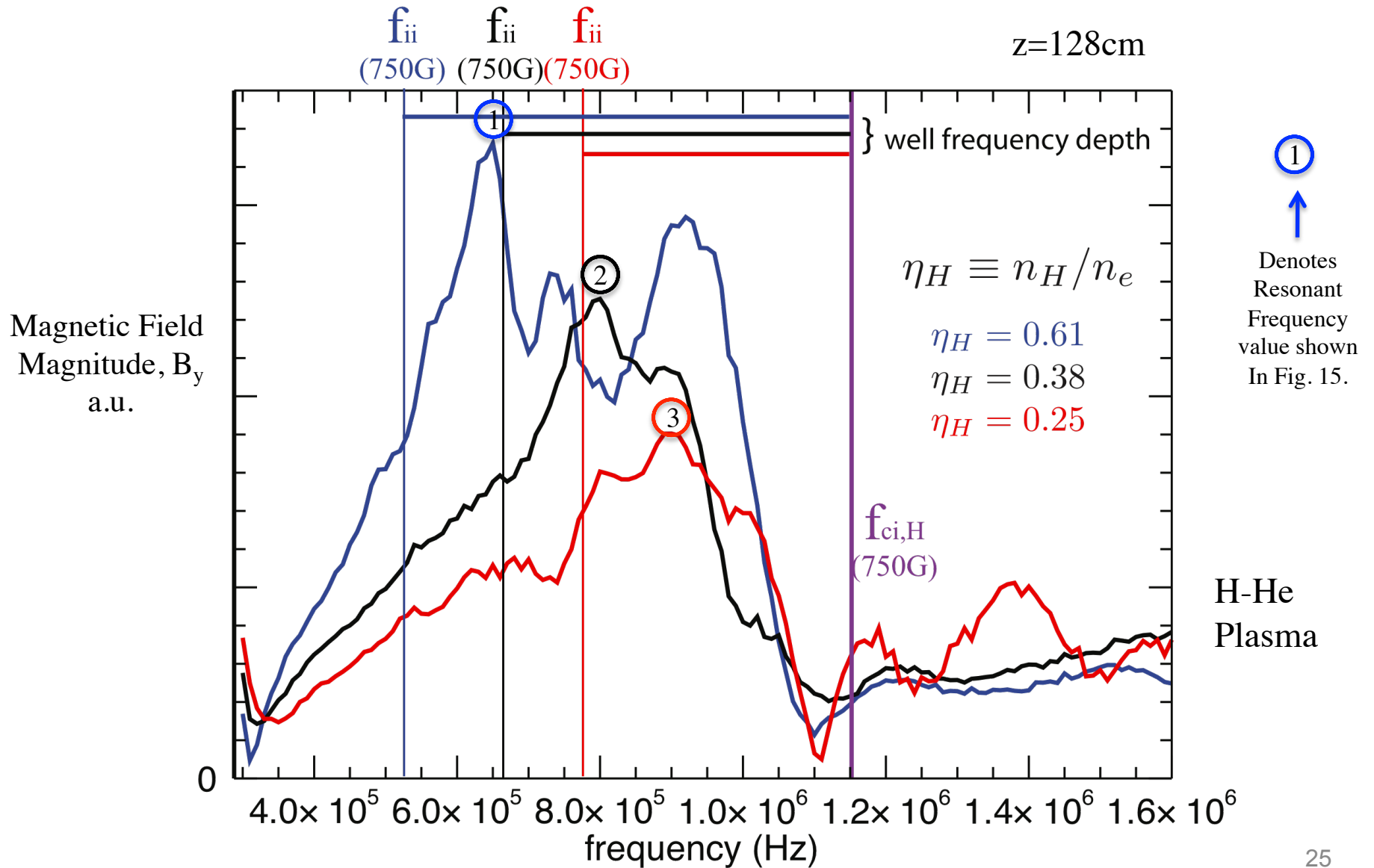
$\eta_H = 0.75$
 $\mu = -0.3$



Magnetic field spectra **measured outside** the magnetic well



Effect of decreasing hydrogen density (at fixed electron density) on magnetic field spectra inside the magnetic well



Perspective on ion-ion hybrid Alfvén wave resonator

- Experimentally have demonstrated that a magnetic step prevents wave penetration into high-field side -- **a necessary condition**
- Pulsed excitation in a magnetic well shows formation of trapped eigenmodes with low “Q” values

Key issues:

- How large is the **dissipation near the ion-ion hybrid** reflection layer ?
- Can an ion beam or a plasma current **trigger maser behavior?**
- **Nonlinear interaction** with ions and electrons

Extra Slides

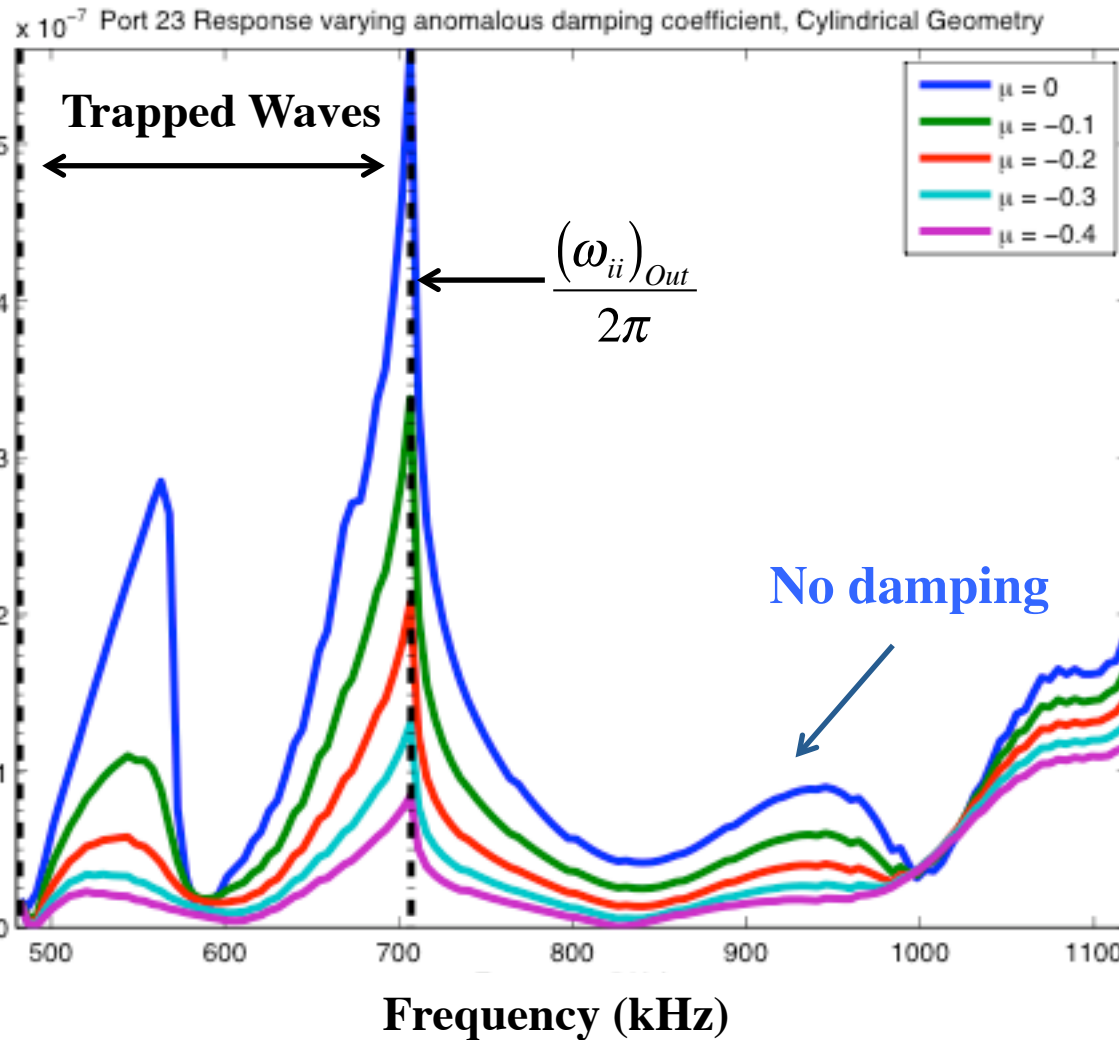
Effect of anomalous damping at reflection layer on spectrum

an effective imaginary part is added to ϵ_{\perp} near reflection point

Theory

Magnitude of wave magnetic field

$$\frac{(\Omega_{He})_{Out}}{2\pi}$$



H-He plasma